Supplementary Information

Harvesting [62]Zn from an aqueous cocktail at the NSCL

Published in 'New Journal of Chemistry'

Katharina A. Domnanich[1,2], Chirag K. Vyas[1,2], E. Paige Abel[1,2], Colton Kalman[1,2], Wesley Walker[1,2], Gregory W. Severin[1,2]

[1] Department of Chemistry, Michigan State University, 578 S Shaw Ln, East Lansing, MI 48824, USA

[2] National Superconducting Cyclotron Laboratory, Michigan State University, 640 S Shaw Ln, East Lansing, MI 48824, USA

e-mail addresses

domnanic@frib.msu.edu, vyas@frib.msu.edu, abelp@nscl.msu.edu, kalman@nscl.msu.edu, walkerw@frib.msu.edu, severin@frib.msu.edu
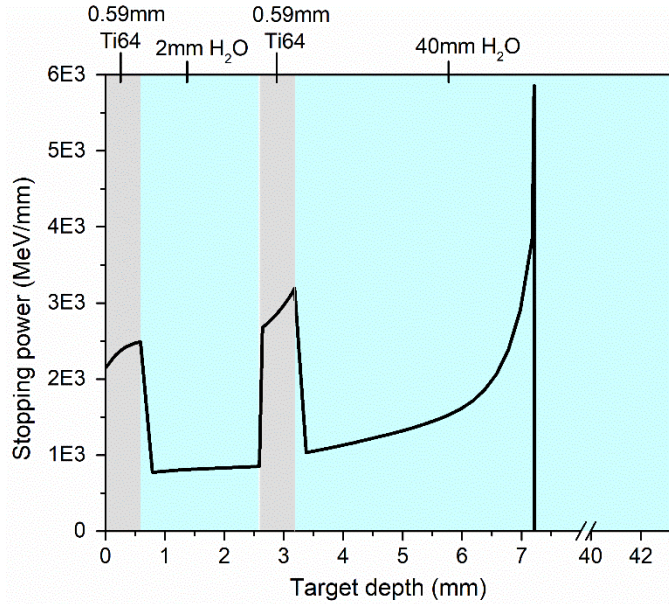
* Corresponding author

Gregory W. Severin

National Superconducting Cyclotron Laboratory

Michigan State University

640 S. Shaw Ln, East Lansing, MI 48824, USA

e-mail: severin@frib.msu.edu

phone:+1-517-353-1087

Fig. S1 The passage of the [78]Kr beam through the different layers of the target. After passing through the Ti64 entrance window, the [78]Kr beam completely traversed the first 2 mm water channel and penetrated 4.1 mm deep into the large water cavity and deposited the majority of its power within the Bragg peak at the end of its path. To estimate the energy of the particles as they travel through the layers of Ti64 and water, the Stopping Range of Ions in Matter compilation (SRIM 2013) was employed.[1]

Radionuclide quantification and comparison with the estimated production

The differential equation determining the number of atoms of a given radionuclide in the water, N_{water}, (which was also observed on the cation exchange column) is given by equation 1:

$$\frac{dN_{water}}{dt} = P * I(t) - k_{ads}N_{water} - \lambda N_{water} \quad (1)$$

where P is the production rate expressed as the number of produced nuclei per incoming [78]Kr nucleus, I(t) represents the beam current at time t (particles/second), k_{ads} is the adsorption rate (s^{-1}) onto the cation exchange column, and λ is the decay constant of the radionuclide (s^{-1}).

The number of atoms of each radionuclide on the cation exchange column, N_{column}, was computed with equation 2:

$$\frac{dN_{column}}{dt} = k_{ads}N_{water} - \lambda N_{column} \quad (2)$$

The radionuclides [7]Be, [24]Na and [62]Zn were selected to obtain a common adsorption rate for cationic species on the cation exchange column. The selection was based on their comparatively high activities, the reliable gamma spectroscopic quantification and their exclusive presence on the cation exchange resin. For this calculation a comparable adsorption of all cationic species is assumed. The Microsoft Excel Solver plug-in was used to find the production rates for [7]Be, [24]Na and [62]Zn (P – values in eq. 1), and a common adsorption rate (k_{ads}). Though the adsorption rate was previously determined in offline

experiments, it was allowed to vary in our model as fitting parameter. This is because k_{ads} is specific for the operation conditions and can vary slightly depending on the experimental settings.

The P for ^7Be, ^{24}Na, ^{62}Zn and their presumed-common k_{ads} were found at the minimized χ^2 difference between the measured activities of the respective radionuclides on the cation exchange resin beds (decay corrected to their retrieval times) and the values produced by equation 2 for the same time points following numerical integration of equations 1 and 2. Since no reliable measurements of the radionuclide levels in the water were available, $N_{water}(t)$ was inferred from the numerical integration of equation 1 using the best-guess k_{ads} and P. The results were then directly applied in equation 2 to calculate the radionuclide levels on the cation exchange resin beds. In the minimized χ^2 calculation the output of equation 2 was compared with the experimentally obtained activity levels of the cation exchange resin beds to obtain an updated k_{ads}.

The resulting k_{ads} allowed to estimate the total quantity of generated radionuclides at EOI ($N_{column} + N_{water}$) from the sum of the activities on the column. The production rates of ^7Be, ^{24}Na and ^{62}Zn were computed with the total quantities of these radionuclides, using the following equation:

$$P = \frac{\lambda(N_{column} + N_{water})}{I(t_{irr}) * (1 - e^{-\lambda * \Delta t_{irr}}) * e^{-\lambda * \Delta t_{EOI}}} \quad (3)$$

where $I(t_{irr})$ represents the average beam current in a certain irradiation segment (particles/second), Δt_{irr} is the duration of the irradiation segment (s) and Δt_{EOI} considers the elapsed time between the irradiation segment and EOI (s). Note: equation 3 expresses the ratio of the actually measured quantity of a radionuclide and the amount that would be produced at a $P = 1$.

The so-obtained P were used in combination with equation 1 and 2 to generate a new k_{ads} for the cation exchange column. With the repeated application of this iterative approach, the most reliable adsorption rate for the cation exchange column was determined. In the following, equation 1 and 2 were used together with k_{ads} to fit the production rates for ^{28}Mg, $^{43,43}K$, ^{61}Cu, and $^{80,83}Sr$, and ^{82m}Rb. To estimate the P of the radionuclides which were adsorbed on at least two components of the system (i.e. $^{44g/m}Sc$, ^{48}V, ^{52}Mn, $^{66,67,68}Ga$, $^{66,69}Ge$, $^{71-74}As$, $^{72,73,75}Se$ and $^{74g/m,75,76,77}Br$) only equation 3 was used with an added N_{res} in the sum of atoms term in the numerator, where N_{res} is the number of atoms elsewhere in the system (e.g. on the anion exchange resin, or on the catalytic converter).

The relationship of a parent/daughter radionuclide pair, such as $^{81}Sr/^{81}Rb$, is described by the Bateman equation, and in combination with equation 1 and 2, the levels of the radioactive daughter ^{81}Rb could be approximated simultaneously in the water and on the column (equation 4 and 5). The parent radionuclide ^{81}Sr and the radioactive daughter ^{81}Rb are assigned subscripts P and D, respectively. The production rates with the minimal χ^2 difference between the measured activities of ^{81}Rb and ^{81}Sr on the cation exchange column and the values produced by equation 2 (for ^{81}Sr) and 5 (for ^{81}Rb) were fitted with the Microsoft Excel solver plug-in.

$$A(t_i)_{D,water} = P_D * I(t_i)\left(1 - e^{-\lambda_D \Delta t}\right) + P_P * I(t_i)\left(1 - e^{-\lambda_D \Delta t}\right) - P_P$$
$$* I(t_i)\left(e^{-\lambda_P \Delta t} - e^{-\lambda_D \Delta t}\right)\frac{\lambda_D}{\lambda_D - \lambda_P} - A(t_{i-1})_{D,water} * e^{-\lambda_D \Delta t} - A(t_{i-1})_{D,water}\, k_{ads}\Delta t$$
$$+ A(t_{i-1})_{P,water}\left(e^{-\lambda_P \Delta t} - e^{-\lambda_D \Delta t}\right)\frac{\lambda_D}{\lambda_D - \lambda_P}$$

$$(4)$$

In equation 4, the activity of ^{81}Rb in the water at time t_i (i.e. $A(t_i)_{D,water}$ in Bq) is given by the beam current-dependent production of ^{81}Sr and ^{81}Rb (first three terms), where Δt represents the time interval between t_i and t_{i-1} (s). The following terms consider the decrease of ^{81}Rb by its decay and the adsorption on the cation exchange column as well as the in-growth by the decay of ^{81}Sr, which depends on the ^{81}Sr activity in the water at the previous time t_{i-1} (i.e. $A(t_{i-1})_{P,water}$).

$$A(t_i)_{D,column} = A(t_{i-1})_{D,water} k_{ads} \Delta t + A(t_{i-1})_{D,column} e^{-\lambda_D \Delta t}$$
$$+ A(t_{i-1})_{P,column} \left(e^{-\lambda_P \Delta t} - e^{-\lambda_D \Delta t} \right) \frac{\lambda_D}{\lambda_D - \lambda_P}$$

(5)

Equation 5 shows that the adsorption of ^{81}Rb from the water (first term) as well as the decay of ^{81}Sr immobilized on the column $A(t)_P$, contribute towards the ^{81}Rb activity on the column at time t_i (i.e. $A(t_i)_{D,column}$ in Bq).

To estimate the error in the adsorption and production rates computed with the minimized chi square approach, the critical values of the χ^2 distribution at a probability range of 0.95 were used. The fitted parameters (k_{ads} and P of a certain radionuclide) were varied until the new χ^2 was increased by the numerical amount of the critical value. The tabulated critical values amounted to 2.9957, 2.6049 and 2.3719, depending if 2, 3 or 4 parameters were fitted within the calculation. The difference between the optimized and the newly computed k_{ads} and P was assigned as error.
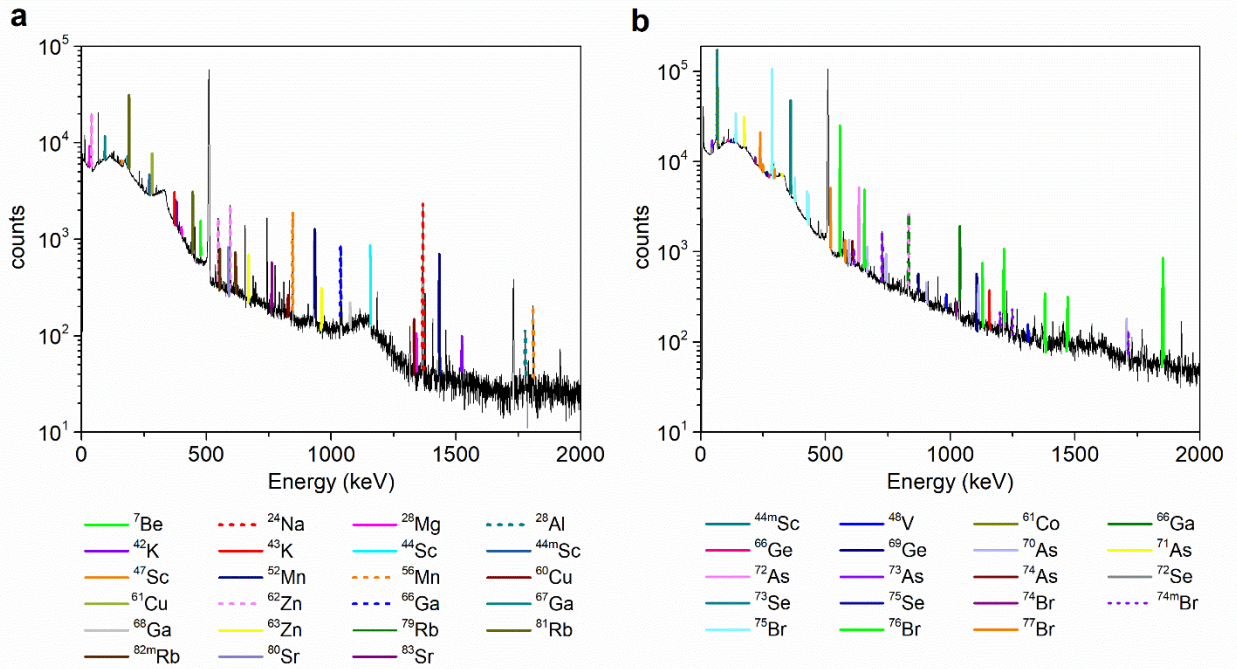
Fig. S2 Gamma spectra of the (**a**) cation and (**b**) anion exchange column directly after retrieving them from the harvesting system.

Table S1 Nuclear data used to quantify the collected radionuclides

The gamma-ray energies were carefully selected to avoid an overlap between different radionuclides. This is the reason why also less intense gamma-rays were considered for the analysis. For the characteristic gamma-rays of ^{28}Mg no uncertainty for the branching ratio was given, therefore an uncertainty of 10% was assumed. The nuclear data was retrieved from the IAEA Nuclear data and decay structure database.[2]

Though the measured samples and components are not considered as standard geometries, no correction factor or additional error were considered. Gamma spectroscopic measurements performed with our system have shown ≤10% difference between a point source and ions adsorbed on a column. In comparison to the statistical counting errors, the influence of different geometries becomes negligible.

Radionuclide	Half-life	Gamma-Ray Energy (keV)	Branching Ratio (%)
^{7}Be	53.22 d	477.6	10.44(4)
^{24}Na	14.997 h	1368.6	99.9936(15)
^{28}Mg	20.92 h	400.6	36(4)
		941.7	36.4
		1342.2	54(5)
^{42}K	12.36 h	1524.6	18.08(9)
^{43}K	22.3 h	372.8	86.8(2)
		396.9	11.85(8)
		593.4	11.26(8)
		617.5	79.2(6)
^{44m}Sc	58.61 h	271.2	86.7(3)
^{48}V	15.97 d	944.1	7.87(7)
		983.5	99.98(4)
		1312.1	98.2(3)
^{52}Mn	5.59 d	744.2	90(12)
		935.5	94.5(13)
		1434.1	100.0(14)
^{56}Mn	2.58 h	846.8	98.85(3)
		1810.7	26.9(4)
^{61}Cu	3.34 h	282.9	12.2(22)
		656.0	10.8(20)
^{62}Zn	9.19 h	40.9	25.5(23)
		548.3	15.3(14)
		596.6	26.0(20)
^{67}Ga	3.26 d	184.6	21.41(1)
		208.9	2.46(1)
		393.5	4.56(24)
^{68}Ga	67.7 min	1077.3	3.22(3)

Radionuclide	Half-life	Gamma-Ray Energy (keV)	Branching Ratio (%)
^{66}Ge	2.26 h	108.9	10.6(4)
		273.0	10.6(4)
		338.1	28.3(15)
		381.9	28.3(15)
		470.6	7.5(4)
^{67}Ge	18.9 min	167.0	84.0(5)
		828.3	3.0(3)
		1472.8	4.9(2)
		1809.6	1.32(16)
^{69}Ge	39.05 h	318.6	1.55(20)
		872.0	11.9(16)
		1106.8	36(4)
^{70}As	52.6 min	668.2	22.1(17)
		743.6	22.1(19)
		905.6	11.2(9)
		1113.6	20.6(16)
		1707.6	17.5(10)
^{71}As	65.3 min	174.9	82.4(20)
		326.8	3.05(8)
		499.9	3.64(9)
		1095.5	4.1(12)
^{72}As	26 h	629.9	8.07(24)
		1050.8	1.00(3)
		1464	1.13(3)
^{73}As	80.3 d	53.4	10.6
^{74}As	17.77 d	595.8	59(3)
^{72}Se	8.4 d	45.9	57.2(4)
^{73}Se	7.15 h	361.2	97.0(10)
		865.1	0.505(20)
^{75}Se	119.8 d	96.7	3.45(2)
		121.1	17.2(12)
		136.0	58.5(4)
		264.7	58.9(4)
^{74}Br	25.4 min	218.9	14.1(19)
		1022.8	5.19(19)
^{74m}Br	46 min	615.2	6.7(7)
		1200.5	5.2(6)
		1249.5	6.7(6)
^{75}Br	96.7 min	141.2	6.6(6)
		286.5	88(5)
		377.4	3.93(23)

Radionuclide	Half-life	Gamma-Ray Energy (keV)	Branching Ratio (%)
^{76}Br	16.2 h	559.1	74.0(20)
		657.0	15.9(9)
		1216.1	8.8(5)
		1853.7	14.7(8)
^{77}Br	57.04 h	239.0	23.1(5)
		249.8	2.98(9)
		520.7	22.4(6)
^{81}Rb	4.57 h	190.5	64.9
		446.2	23.5(9)
^{82m}Rb	6.47 h	554.4	62.4(9)
		619.1	37.98(9)
		698.4	26.3(7)
		1044.1	32.08(8)
^{80}Sr	1.77 h	175	10.1(14)
		589	39(5)
^{81}Sr	22.3 min	147.8	30(4)
		188.3	15.4(19)
		443.3	17.5(22)
^{83}Sr	32.4 min	381.5	14 (11)
		762.7	26.7(22)

Table S2 Activities of radioactive species (related to the EOI) determined exclusively on the cation exchange column

| Radionuclide	A_{EOI} (kBq) in April	A_{EOI} (kBq) in May
^{7}Be	183.7(60)	334.5(110)
^{24}Na	251.4(80)	366.3(60)
^{28}Mg	12.8(10)	20.6(10)
^{42}K	34.1(40)	60.9(40)
^{43}K	22.4(6)	39.3(10)
^{61}Cu	631.6(480)	769.1(580)
^{62}Zn	280.4(110)	412.4(150)
^{82m}Rb	28.6(10)	37.9(10)
^{80}Sr	187.2(370)	161.8(110)
^{81}Sr	95.5(100)	133.9(140)
^{83}Sr	73.7(40)	125.7(60)

Table S3 Activities of radioactive species (related to the EOI) determined on the cation- (Cat$^+$X) and/or anion (An$^-$X) column and on the catalytic converter (KLC)

Radionuclide	A$_{EOI}$ (kBq) in April			A$_{EOI}$ (kBq) in May		
	KLC	Cat$^+$X	An$^-$X	KLC	Cat$^+$X	An$^-$X
^{44m}Sc	3.8(2)	9.4(6)	62.5(46)	14.9(10)	23.2(10)	92.2(30)
^{52}Mn	2.7(2)	69.8(14)	-	3.9(3)	112.8(13)	-
^{48}V	3.9(2)	-	21.4(6)	12.8(5)	-	36.4(10)
^{67}Ga	51.6(14)	38.1(19)	270.9(35)	106.0(32)	69.8(29)	358.6(42)
^{69}Ge	163.9(67)	-	661.7(271)	359.7(221)	-	1392.3(480)
^{71}As	109.8(25)	-	653.2(142)	213.0(96)	-	1401.4(278)
^{72}Se	-	-	149.3(23)		-	220.4(36)
^{73}Se	225.9(36)	-	1953.7(578)	137.8(24)		10871(1510)
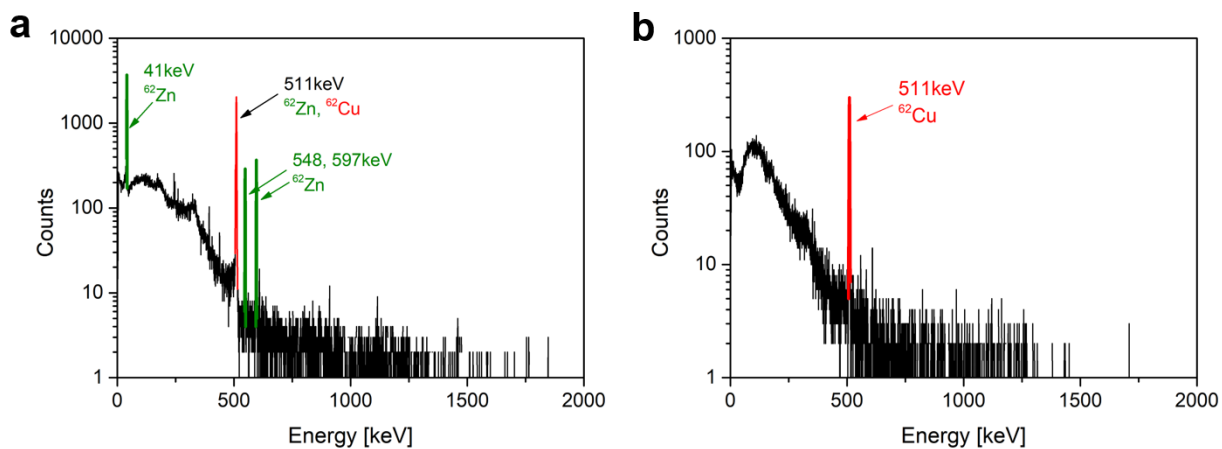
Fig. S3 Gamma spectra (**a**) of the AG1x8 column after removal of all initially present radionuclidic contaminants, with ^{62}Zn and the in-grown ^{62}Cu being the only adsorbed radionuclides and (**b**) the pure ^{62}Cu eluate of sample 2.
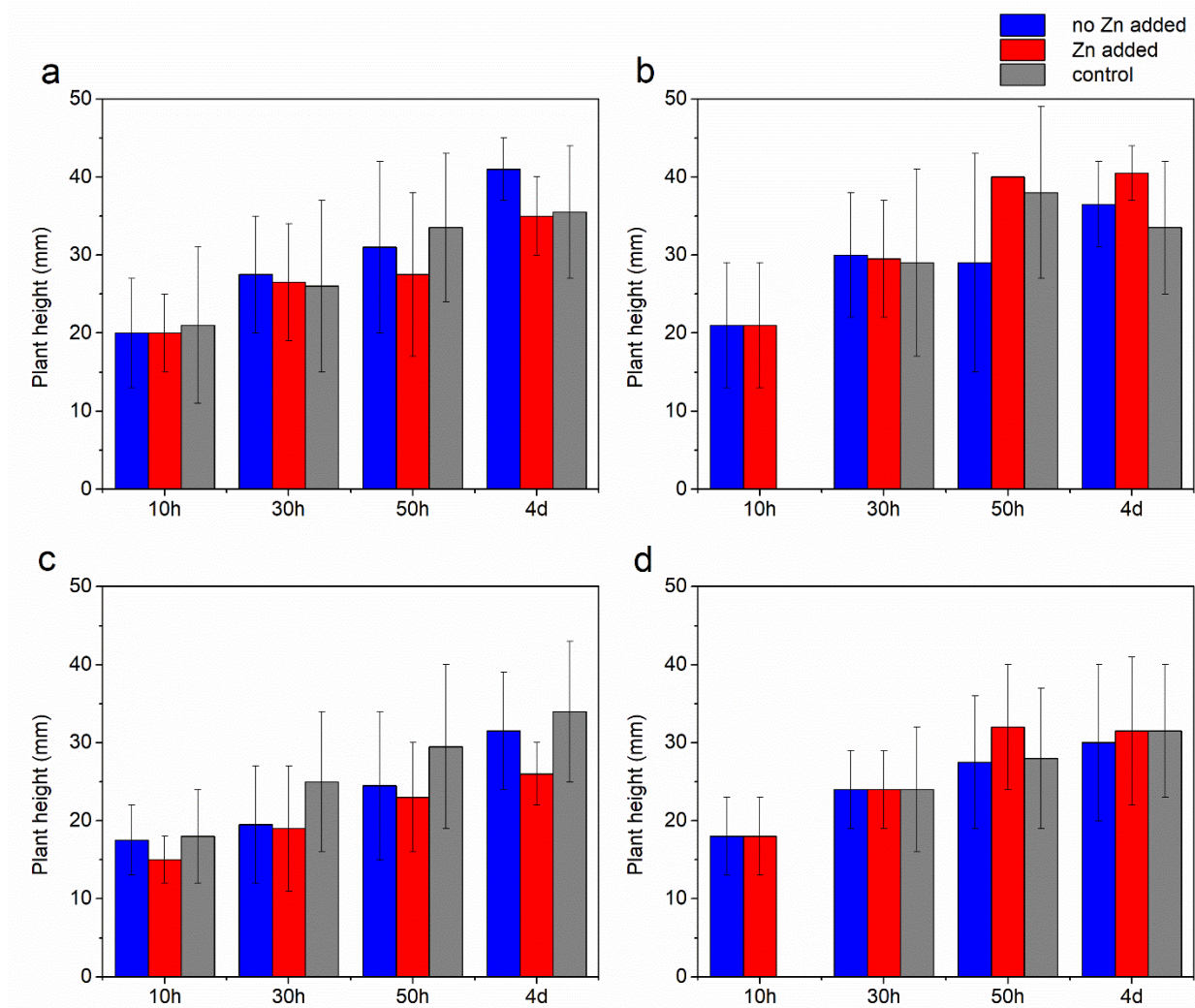
Fig. S4 The growth of garden cress plants (**a** and **b**) cultivated on a cotton layer and (**c** and **d**) in water over the duration of the uptake experiment. The garden cress plants were incubated with (**a** and **c**) ligand-free and (**b** and **d**) DTPA-radiolabelled ^{62}Zn. An analogous solution, only deficient in ^{62}Zn, was used for the incubation of the control dishes. The bars indicate the variation in plant height (n≥3) within one dish.

References

1   J. P. Ziegler, J.F.; Ziegler, M.D; Biersack, 2013.

2   International Atomic Energy Agency, Nuclear Data Services, https://www-nds.iaea.org/, (accessed 23 April 2020).